

Dinuclear Asymmetric Ruthenium Complexes with 5-Cyano-1,10-phenanthroline as a Bridging Ligand†

María G. Mellace,[‡] Florencia Fagalde,[‡] Néstor E. Katz,^{*,‡} Irma G. Crivelli,[§] Alvaro Delgadillo,^{||} Ana María Leiva,^{||} Bárbara Loeb,^{||} María Teresa Garland,[⊥] and Ricardo Baggio[#]

Instituto de Química Física, Facultad de Bioquímica, Química y Farmacia, Universidad Nacional de Tucumán, Ayacucho 491, (T4000INI) San Miguel de Tucumán, Republic of Argentina, Departamento de Química, Facultad de Ciencias, Universidad de Chile, Casilla 653, Santiago, Chile, Facultad de Química, Pontificia Universidad Católica de Chile, Casilla 306, Santiago, Chile, Departamento de Física, Facultad de Ciencias Físicas y Matemáticas, Universidad de Chile and CIMAT, Casilla 407, Santiago, Chile, and Departamento de Física, Comisión Nacional de Energía Atómica (CONEA), Av. Gral Paz 1499, 1650 San Martín, Pcia. de Buenos Aires, Republic of Argentina

Received October 17, 2003

New dinuclear asymmetric ruthenium complexes of the type $[(bpy)_2Ru(5-CNphen)Ru(NH_3)_5]^{4+/5+}$ ($bpy = 2,2'$ -bipyridine; $5-CNphen = 5$ -cyano-1,10-phenanthroline) have been synthesized and characterized by spectroscopic, electrochemical, and photophysical techniques. The structure of the cation $[(bpy)_2Ru(5-CNphen)Ru(NH_3)_5]^{4+}$ has been determined by X-ray diffraction. The mononuclear precursor $[Ru(bpy)_2(5-CNphen)]^{2+}$ has also been prepared and studied; while its properties as a photosensitizer are similar to those of $[Ru(bpy)_3]^{2+}$, its luminescence at room temperature is quenched by a factor of 5 in the mixed-valent species $[(bpy)_2Ru^{II}(5-CNphen)Ru^{III}(NH_3)_5]^{5+}$, pointing to the occurrence of intramolecular electron-transfer processes that follow light excitation. From spectral data for the metal-to-metal charge-transfer transition $Ru^{II} \rightarrow Ru^{III}$ in this latter complex, a slight electronic interaction ($H_{AB} = 190 \text{ cm}^{-1}$) is disclosed between both metallic centers through the bridging 5-CNphen.

Ruthenium polypyridine complexes have been extensively studied due to their applications in artificial photosynthesis.¹ However, few studies have included substituted phenanthrolines as bridging ligands. The rigidity of 1,10-phenanthroline lends interesting properties to those photosensitizers incorporating its structure, such as long lifetimes for the metal-to-ligand charge transfer (MLCT) excited states, a relevant factor in the design of efficient photocatalysts.² On the other

hand, the preparation of metallic dendrimers leads to important applications in molecular carriers in chemical and biochemical systems.³

We report in this work new mono- and dinuclear ruthenium complexes that incorporate 5-cyano-1,10-phenanthroline (=5-CNphen) as a bridging ligand and 2,2'-bipyridine (=bpy) as an auxiliary ligand. The new asymmetric mixed-valent species described in this work can be used as a model for testing current electron transfer theories.⁴ The structures of bpy and 5-CNphen are shown in Chart 1.

Experimental Section

Materials. All chemicals used in this work were analytical-reagent grade and employed as supplied, without further purification, except for acetonitrile, which was dried and stored over 4 Å

* To whom correspondence should be addressed. E-mail: nkatz@arnet.com.ar.

† Presented in part at the XIII Congreso Argentino de Fisicoquímica y Química Inorgánica, Bahía Blanca, Argentina, April 2003.

‡ Universidad Nacional de Tucumán.

§ Facultad de Ciencias, Universidad de Chile.

|| Pontificia Universidad Católica de Chile.

⊥ Facultad de Ciencias Físicas y Matemáticas, Universidad de Chile.

CONEA.

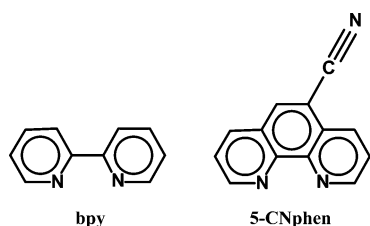
- (1) (a) Sutin, N.; Creutz, C. *Pure Appl. Chem.* **1980**, *52*, 2717. (b) Meyer, T. J. *Acc. Chem. Res.* **1989**, *22*, 163. (c) Balzani, V.; Scandola, F. *Supramolecular Photochemistry*; Ellis Horwood: Chichester, U.K., 1991. (d) Balzani, V.; Juris, A.; Venturi, M.; Campagna, S.; Serroni, S. *Chem. Rev.* **1996**, *96*, 759. (e) Balzani, V.; Campagna, S.; Denti, G.; Juris, A.; Serroni, S.; Venturi, M. *Acc. Chem. Res.* **1998**, *31*, 26. (f) Dürr, H.; Bossmann, S. *Acc. Chem. Res.* **2001**, *34*, 905.

- (2) Treadway, A.; Loeb, B.; López, R.; Keene, F. R.; Anderson, P.; Meyer, T. J. *Inorg. Chem.* **1996**, *35*, 2242.

- (3) Calderazzo, F.; Pampaloni, G.; Passarelli, V. *Inorg. Chim. Acta* **2002**, *330*, 136. (b) Kim, M.-J.; Konduri, R.; Ye, H.; MacDonnell, F.; Puntoriero, F.; Serroni, S.; Campagna, S.; Holder, T.; Kinsel, G.; Rajeshwar, K. *Inorg. Chem.* **2002**, *41*, 2471.

- (4) (a) Fagalde, F.; Katz, N. E. *Polyhedron* **1995**, *14*, 1213. (b) Mellace, M. G.; Fagalde, F.; Katz, N. E. *Polyhedron* **2003**, *22*, 369.

Chart 1



molecular sieves for the electrochemical and luminescence measurements.

Instrumentation and Measurements. ^1H NMR and COSY spectra were obtained on Bruker AVANCE 400 and Bruker ACP200 spectrometers, all spectra being referred to TMS as an internal standard. UV–visible absorption spectra were recorded on a Shimadzu UV-160 A instrument, using 1-cm quartz cells. Infrared spectra were obtained as KBr pellets, with a double-beam Perkin-Elmer 983G IR spectrometer and a Bruker VECTOR 22 FTIR spectrometer. Fluorescence measurements were performed with a Shimadzu RF 5301 PC spectrofluorometer, provided with 1-cm fluorescence cells. The solutions were purged with Ar for 10 min before each photophysical measurement. Electrochemistry experiments were carried out with a BAS CV-50 W version 2-3 MF 9093 voltammetric analyzer and EQMAT cyclic voltammetry equipment, using an H-type cell, with a conventional three-electrode array, consisting of a platinum working electrode, a platinum wire as the auxiliary electrode, and a Ag/AgCl (3 M KCl) or SCE as reference electrode. All solutions were prepared in acetonitrile, with 0.1 M TBAH (tetrakis-*n*-butylammonium hexafluorophosphate) as the supporting electrolyte, and thoroughly degassed with Ar, prior to each experiment. Working and auxiliary electrodes were polished with a suspension of alumina (0.05 μm) in acetonitrile. Cyclic voltammograms were run at a sweep rate of 200 $\text{mV}\cdot\text{s}^{-1}$. The reported $E_{1/2}$ values were calculated as the semidifference between the E_p corresponding to the cathodic and anodic waves: $E_{1/2} = (E_c + E_a)/2$. The potential values reported in this work are referred vs SCE. Chemical analyses were carried out at INQUIMAE, University of Buenos Aires, Buenos Aires, Argentina, and at the Pontificia Universidad Católica de Chile. X-ray diffraction measurements were performed in a Bruker Smart Apex diffractometer equipped with a CCD area detector, using graphite-monochromatized, Mo K α radiation from a fine-focus sealed tube. The specimen used was an orange plate, 0.32 \times 0.12 \times 0.02 mm^3 .

Syntheses. All complexes were protected from light during syntheses and measurements. The ligand 5-cyano-1,10-phenanthroline was synthesized by following procedures reported in the literature,⁵ by first obtaining the 1,10-phenanthroline 5,6-epoxide as an intermediate product. The precursor complex *cis*-Ru(bpy) $_2\text{Cl}_2\cdot 2\text{H}_2\text{O}$ was obtained according to known methods.⁶

Preparation of [Ru(bpy) $_2$ (5-CNphen)](PF $_6$) $_2\cdot \text{H}_2\text{O}$ (1). A solution of *cis*-Ru(bpy) $_2\text{Cl}_2\cdot 2\text{H}_2\text{O}$ (250 mg, 0.48 mmol) in CH_3OH (50 mL) was deaerated with Ar for 30 min at room temperature. 5-CNphen (100 mg, 0.49 mmol) was then added, and the mixture was refluxed under Ar for 5 h, a period during which the solution changed from purple to reddish-orange. After the reaction time was completed, the solution was evaporated to ca. 8 mL and a concentrated solution of NH_4PF_6 (2 g in 20 mL of H_2O) was added. The final mixture was stored in the refrigerator overnight. The red-

orange solid formed was filtered out, washed with water, ethanol, and ether, redissolved in a minimum volume of acetonitrile, and passed down an alumina column, previously equilibrated with a CH_3CN /toluene (1:2 v/v) mixture. The middle portion of the orange band eluted with CH_3CN was collected, concentrated to ca. 5 mL under reduced pressure, cooled, and reprecipitated with NH_4PF_6 (2 g/20 mL of H_2O). The orange solid was filtered out, washed with small volumes of cold water, then with ethanol, and finally with ether, dried, and stored under vacuum over P_4O_{10} for 1 day. Yield: 237 mg, 54%. Anal. Found (mean of 3 determinations): C, 42.4; N, 10.5; H, 2.7. Calcd for $\text{C}_{33}\text{H}_{25}\text{N}_7\text{P}_2\text{O}_2\text{F}_{12}\text{Ru}$: C, 42.8; N, 10.6; H, 2.7. ^1H NMR (CD_3CN ; δ (ppm)) of the 5-CN-phen ring: 8.88 (s, 1H, H $_6$); 8.80 (dd, 1H, $J_{3-4} = 8.31$ Hz, H $_4$); 8.70 (dd, 1H, H $_7$); 8.25 (dd, 1H, $J_{2-3} = 5.38$ Hz; $J_{2-4} = 1.22$ Hz, H $_2$); 8.23 (dd, 1H, H $_9$); 7.90 (m, 1H, H $_3$), 7.84 (m, 1H, H $_8$). ^1H NMR (CD_3CN ; δ (ppm)) of the 2,2'-bpy rings: 8.56 (dd, 2H, $J_{c-d} = 8.07$ Hz, H $_d$); 8.52 (dd, 2H, H $_d'$); 8.13 (t, 2H, H $_c$); 8.03 (t, 2H, H $_c'$); 7.85 (m, 2H, H $_a$); 7.54 (dd, 2H, H $_a'$); 7.48 (2H, t, $J_{a-b} = 4.89$ Hz, $J_{c-b} = 7.82$ Hz, H $_b$); 7.25 (m, 2H, H $_b'$).

Preparation of [Ru(bpy) $_2$ (5-CNphen)Ru(NH $_3$) $_5$](PF $_6$) $_4\cdot 10\text{H}_2\text{O}$ (2). A solution of **1** (56 mg, 0.061 mmol) in acetone (14 mL) was purged with Ar for 30 min. [Ru(NH $_3$) $_5$ (H_2O)](PF $_6$) $_2$ (35.6 mg; 0.074 mmol), prepared as in ref 7, was added, and the resulting mixture was stirred under Ar for 4 h. The dark-red solution was concentrated to half-volume, and a solution of NH_4PF_6 (2 g in 20 mL of H_2O) was added to induce precipitation. After storage for 24 h in the refrigerator, the solid was filtered out and rinsed and purified by chromatography in alumina as for complex **1**. The unreacted mononuclear precursor eluted first, while the new dinuclear complex was collected with a solution of NH_4PF_6 in MeOH (1 g in 100 mL), rotoevaporated to ca. 5 mL, and precipitated with a solution of NH_4PF_6 (2 g/20 mL of H_2O). Isolation and drying of the pure solid was performed as for complex **1**. Yield: 70 mg, 82%. Anal. Found: C, 25.7; N, 9.8; H, 3.4. Calcd for $\text{C}_{33}\text{H}_{58}\text{N}_{12}\text{O}_{10}\text{P}_4\text{F}_{24}\text{Ru}_2$: C, 25.3; N, 10.7; H, 3.7. Crystals suitable for X-ray diffraction studies were obtained by slow diffusion of ether (1.5 mL) into a concentrated solution of the complex (13 mg) in acetone (1.5 mL). ^1H NMR (CD_3CN ; δ (ppm)) of the 5-CNphen ring: 8.88 (dd, 1H, $J_{3-4} = 8.38$ Hz, H $_4$); 8.79 (s, 1H, H $_6$); 8.66 (dd, 1H, H $_7$); 8.21 (dd, 1H, $J_{2-3} = 5.28$ Hz; $J_{2-4} = 1.06$ Hz, H $_2$); 8.17 (dd, 1H, H $_9$); 7.80 (m, 1H, H $_8$). ^1H NMR (CD_3CN ; δ (ppm)) of the 2,2'-bpy rings: 8.57 (dd, 2H, H $_d$); 8.52 (dd, 2H, H $_d'$); 8.14 (m, 2H, H $_c$); 8.03 (c, 2H, H $_c'$); 7.87 (m, 2H, H $_a$); 7.57 (m, 2H, H $_a'$); 7.48 (m, 2H, H $_b$); 7.26 (c, 2H, H $_b'$).

Preparation of [Ru $^{\text{II}}$ (bpy) $_2$ (5-CNphen)Ru $^{\text{III}}$ (NH $_3$) $_5$](PF $_6$) $_5$ (3). The mixed-valent complex was prepared by adding with a glass syringe 5 mL of Br_2 to a solution of the dinuclear precursor **2** (40 mg, 0.03 mmol) and 1 equiv (12 mg, 0.035 mmol) of TBAH in 20 mL of acetonitrile. The solution changed from reddish-orange to yellow. After concentration to ca. 10 mL, the new complex was precipitated with ether (100 mL) and stored 24 h in the freezer. The orange salt (**3**) was filtered out, washed with cold ether, and dried under vacuum over P_4O_{10} . Yield: 33 mg, 75%. Anal. Found: C, 26.3; N, 9.5; H, 3.2. Calcd for $\text{C}_{33}\text{H}_{38}\text{N}_{12}\text{P}_5\text{F}_{30}\text{Ru}_2$: C, 25.9; N, 10.9; H, 2.5.

Results and Discussion

Syntheses. The new complexes synthesized are soluble in acetone and acetonitrile but only partially soluble in water and ethanol. Elemental analyses and ^1H NMR spectra confirmed the purity of the complexes.

(5) (a) Krishnan, S.; Kuhn, D. G.; Hamilton, G. A. *J. Am. Chem. Soc.* **1977**, *99*, 8121. (b) Shen, Y.; Sullivan, B. P. *Inorg. Chem.* **1995**, *34*, 6235.

(6) Sullivan, B. P.; Salmon, D. J.; Meyer, T. J. *Inorg. Chem.* **1978**, *17*, 3334.

(7) Sutton, J. E.; Taube, H. *Inorg. Chem.* **1981**, *20*, 3125.

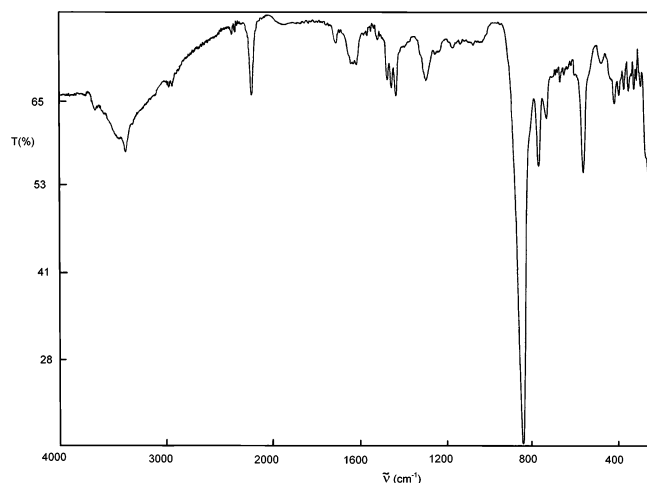


Figure 1. IR spectrum of $[\text{Ru}(\text{bpy})_2(5\text{-CNphen})\text{Ru}(\text{NH}_3)_5](\text{PF}_6)_4 \cdot 10\text{H}_2\text{O}$ (KBr pellet).

Infrared Spectroscopy. The IR spectra of the new complexes **1–3** presented distinctive features in the 2250–2150 cm^{-1} region, where the $\text{C}\equiv\text{N}$ stretching band of the nitrile group, $\nu(\text{C}\equiv\text{N})$, occurs. A single band at 2222 cm^{-1} was assignable to this mode in the free ligand, while coordination to the ruthenium atom of the $\text{Ru}^{\text{II}}(\text{bpy})_2$ moiety (Ru_b) through N1 and N10 of 5-CNphen in the mononuclear complex **1** shifted this band toward higher frequency [$\nu(\text{C}\equiv\text{N}) = 2231 \text{ cm}^{-1}$]. Coordination of the nitrile group of 5-CNphen to the ruthenium atom of the $\text{Ru}^{\text{II}}(\text{NH}_3)_5$ moiety (Ru_a) produced instead a single, intense band at $\nu(\text{C}\equiv\text{N}) = 2182 \text{ cm}^{-1}$ in the dinuclear complex **2**, as shown in Figure 1. This strong negative shift with respect to the free ligand value ($\Delta\nu = -40 \text{ cm}^{-1}$) can be attributed to the important π -back-bonding effect of the pentaammineruthenium(II) group, as previously observed for other nitrile-coordinated ruthenium complexes.⁸ In complex **3**, where π -back-bonding is inoperative, the value observed, $\nu(\text{C}\equiv\text{N}) = 2231 \text{ cm}^{-1}$, was identical with that of the mononuclear species **1**. Additional evidence of coordination to the pentaammineruthenium group in both dinuclear complexes was provided by the values of the ammonia symmetric deformation modes, $\delta_{\text{sym}}(\text{NH}_3)$, observed at 1286 cm^{-1} in complex **2** (see Figure 1) and at 1303 cm^{-1} in complex **3**, characteristic of localized oxidation states II and III, respectively, for the capping Ru_a , as already observed for several ammineruthenium complexes.⁹

UV–Visible Spectroscopy. The electronic absorption spectra of complexes **1–3** in acetonitrile, displayed in Table 1, revealed in all cases composite-broad bands. In complex **1**, both intense absorption bands at $\lambda_{\text{max}} = 449$ and 419 nm can be assigned to mixed $d_\pi(\text{Ru}_\text{b}) \rightarrow \pi^*(\text{bpy})$ and $d_\pi(\text{Ru}_\text{b}) \rightarrow \pi^*(5\text{-CNphen})$ MLCT transitions. Strong absorption bands, corresponding to the $\pi \rightarrow \pi^*$ transitions of the polypyridine ligands,¹⁰ were observed between 200 and 300 nm. Complex **2** presented the same MLCT bands slightly shifted to $\lambda_{\text{max}} = 454$ and 418 nm, along with a second

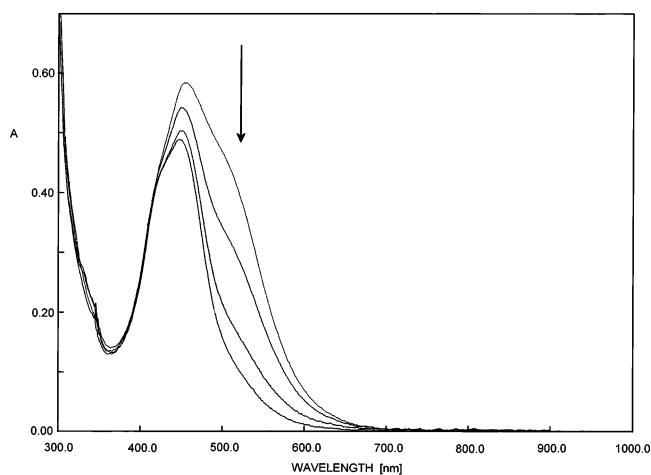


Figure 2. Spectrophotometric titration of $[(\text{bpy})_2\text{Ru}^{\text{II}}(5\text{-CNphen})\text{Ru}^{\text{II}}(\text{NH}_3)_5]^{4+}$ by Br_2 , in CH_3CN ($C = 4.5 \times 10^{-5} \text{ M}$), with increasing amounts of oxidant in molar ratios $[\text{Ru}]/[\text{Br}_2] = 1/0, 1/0.5, 1/1$, and $1/1.25$, in the arrow direction. $T = 22^\circ\text{C}$.

Table 1. Electronic Absorption Data of 5-CNphen Complexes of Ruthenium in CH_3CN , at Room Temperature

complex	λ_{max} , nm ($10^{-3}\epsilon_{\text{max}}$, $\text{M}^{-1}\text{cm}^{-1}$)
$[\text{Ru}(\text{bpy})_2(5\text{-CNphen})]^{2+}$	449 (9.5)
	419 (7.9)
	331 (sh)
	284 (38)
	266 (36)
	232 (35)
	208 (31)
	500 (9.0)
$[\text{Ru}(\text{bpy})_2(5\text{-CNphen})\text{Ru}(\text{NH}_3)_5]^{4+}$	454 (13)
	418 (9.0)
	284 (40)
	266 (40)
	233 (25)
	208 (25)
	664 (0.08)
	449 (10)
$[\text{Ru}(\text{bpy})_2(5\text{-CNphen})\text{Ru}(\text{NH}_3)_5]^{5+}$	419 (8.2)
	284 (36)
	265 (30)
	232 (25)
	210 (32)

intense band at $\lambda_{\text{max}} \approx 500 \text{ nm}$ (value obtained by Gaussian deconvolution), attributed to $d_\pi(\text{Ru}_\text{a}) \rightarrow \pi^*(5\text{-CNphen})$ MLCT. This observed value is strongly shifted to lower energies respect to the mononuclear species $[\text{Ru}(\text{NH}_3)_5(\text{NCPH})]^{2+}$ (with $\text{PhCN} = \text{benzonitrile}$), $\lambda_{\text{max}} = 376 \text{ nm}$,⁹ due to the electron-withdrawing effects of the pyridine rings and the second metallic center.

A redox spectrophotometric titration of complex **2** with Br_2 in CH_3CN (standardized by using $\epsilon = 183 \text{ M}^{-1}\text{cm}^{-1}$ at 392 nm),¹⁰ shown in Figure 2, caused the band at 500 nm to disappear. Simultaneously, a new weak band generated at $\lambda_{\text{max}} = 664 \text{ nm}$ (with $\epsilon_{\text{max}} = 80 \text{ M}^{-1}\text{cm}^{-1}$ and bandwidth $\Delta\nu_{1/2} = 6300 \text{ cm}^{-1}$; all values obtained by Gaussian deconvolution), shown in Figure 3 for a concentrated solution of **2** to which Br_2 vapor was added, was assigned to a metal-to-metal charge transfer (MMCT), $\text{Ru}_\text{b}^{\text{II}} \rightarrow \text{Ru}_\text{a}^{\text{III}}$, for the new mixed-valent species formed, complex **3**. Similar results were obtained by chemical oxidation with the addition of 1 equiv of a $\text{Ce}(\text{IV})$ salt. The reverse process (reduction of the Ru_a center), with the consequent regeneration of the band at 500

(8) Ford, P. C. *Coord. Chem. Rev.* **1970**, *5*, 75.

(9) Clarke, R. E.; Ford, P. C. *Inorg. Chem.* **1970**, *9*, 227.

(10) Powers, M. J.; Callahan, R. W.; Shanon, D. J.; Meyer, T. J. *Inorg. Chem.* **1976**, *15*, 894.

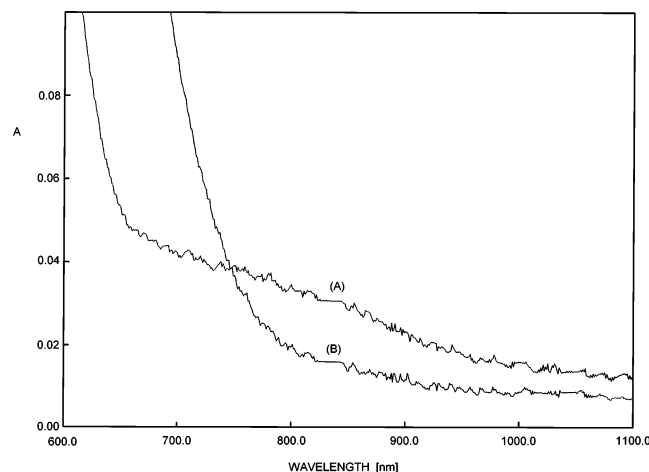


Figure 3. (A) Visible spectrum of $[(bpy)_2Ru^{II}(5-CNphen)Ru^{III}(NH_3)_5]^{5+}$, $C = 5 \times 10^{-4}$ M, in CH_3CN . The spectrum of $[(bpy)_2Ru^{II}(5-CNphen)-Ru^{II}(NH_3)_5]^{4+}$ at the same C is shown in (B) for comparison. $T = 22^\circ C$.

Table 2. Half-Wave Potentials $E_{1/2}$ (V) of the 5-CNphen Complexes of Ruthenium in CH_3CN , vs SCE, at Room Temperature

complex	process	$E_{1/2}$ (V) (ΔE_p , mV)
$[Ru(bpy)_2(5-CNphen)]^{2+}$	$Ru^{III/II}$	1.37 (62)
	$L^{0/-}$	-0.99 (55), -1.41 (63)
$[Ru(bpy)_2(5-CNphen)Ru(NH_3)_5]^{4+}$	$Ru_b^{III/II}$	1.38 (67)
	$Ru_a^{III/II}$	0.68 (67)
	$L^{0/-}$	-1.05 (90), -1.41 (62)

nm and the disappearance of that at 664 nm, was accomplished by adding a spatula tip of $SnCl_2$ to a solution of the oxidized complex in CH_3CN .

The UV–visible spectrum recorded for a solution of the mixed-valent complex **3** in CH_3CN , as shown in Table 1, supported the data obtained by the “in situ” oxidation of complex **2**, as shown in Figure 3. Furthermore, the addition of 1 equiv of a Ce(IV) salt to this compound produced the fully oxidized moiety, $[Ru_b^{III}, Ru_a^{III}]$, where the MMCT and MLCT bands, at 664 and 449 nm respectively, were no longer detectable.

Electrochemical Measurements. The electrochemical properties of complexes **1** and **2** were studied by cyclic voltammetry (CV), in acetonitrile solutions, with 0.1 M TBAH. The $E_{1/2}$ and ΔE_p values obtained in each case are shown in Table 2.

The oxidative range of potentials showed a reversible redox wave at $E_{1/2} = 1.37$ V, associated with the Ru^{III}/Ru^{II} couple for complex **1**, whereas two reversible waves, one at $E_{1/2}^{(1)} = 1.38$ V (assigned to the couple Ru_b^{III}/Ru_b^{II}) and a second one at $E_{1/2}^{(2)} = 0.68$ V (corresponding to the couple Ru_a^{III}/Ru_a^{II}), were determined for the dinuclear complex **2**. The intensities of both waves reflect the relation $[Ru_a]/[Ru_b] = 1$.

Considering the fact that phenanthroline ligands stabilize the oxidation state (II) of Ru, the metal-centered oxidation potentials are slightly more positive than that of the reference complex $[Ru(bpy)_3]^{2+}$ (1.26 V).¹¹ The second oxidative wave is similar to that observed in nitrile-coordinated pentaam-

mineruthenium(II) complexes.¹² The difference of redox potentials, $\Delta E_{1/2}$, determined as $\Delta E_{1/2} = [E_{1/2}(Ru_b^{III}/Ru_b^{II}) - E_{1/2}(Ru_a^{III}/Ru_a^{II})]$, was $\Delta E_{1/2} = 0.70$ V. In both complexes, **1** and **2**, the first reduction potential at $E_{1/2} \approx -1$ V can be assigned to the reduction of 5-CNphen, while the second one at $E_{1/2} = -1.41$ V can be assigned to the first reduction of bpy, by comparison with similar systems.¹¹

X-ray Structure Determination. A highly redundant data set was collected at room temperature up to a $2\theta_{max}$ of ca. 58° and a 0.3° separation between frames. Data integration was performed using SAINT and a multiscan absorption correction applied using SADABS, both programs in the diffractometer package. The structure was solved by direct methods and difference Fourier and refined by least squares on F^2 . All four independent PF_6^- groups showed rotational disorder around the central P atoms and were refined with a split model where the unique central atom presents full occupancy. Anisotropic displacement parameters were used for all ordered, non-H atoms, while an overall isotropic factor was used for all fluorine ions. Hydrogen atoms were placed at their calculated positions and allowed to ride onto their host carbons both in coordinates as well as in thermal parameters. Those corresponding to terminal NH_3 were allowed to rotate as well. All calculations to solve the structure, refine the model proposed, and obtain derived results were carried out with the computer programs SHELXS97 and SHELXL97¹³ and SHELXTL/PC.¹⁴ Full use of the CCDC package was also made for searching in the CSD Database.¹⁵ A survey of crystallographic and refinement data is presented in Table 3, while Table 4 shows relevant interatomic distances and angles and Table 5 (Supporting Information) presents H-bonding interactions.

The structure consists of dinuclear $[(bpy)_2Ru_b(phenCN)-Ru_a(NH_3)_5]^{4+}$ centers (with $Ru_a = Ru1$ and $Ru_b = Ru2$) counterbalanced by four highly disordered PF_6^- anions, as shown in Figure 4. Both RuN_6 coordination polyhedra are octahedral, with the one involving the dinitrogenated bases having been more deformed due to the strain imposed by ligand chelation. The effect is clearly visible in the N–Ru–N coordination angles, with expected $90/180^\circ$ angles displaying a large span ($77.3\text{--}99.3/173.7\text{--}175.0^\circ$) around Ru1 and a much tighter one ($88.0\text{--}92.5/178.3\text{--}179.8^\circ$) around Ru2. The difference is also noticeable in the dihedral angles between N–Ru–N coordination planes: in the former octahedron the planes (which are almost parallel to the planar groups which determine them) subtend to each other angles which range from 79.8 to 96.0° , in contrast to the tighter span of $88.1\text{--}90.1^\circ$ found in the latter. In both polyhedra, coordination distances of equivalent nitrogens are rather even; thus, around Ru1 the mean value is $2.058(21)$ Å for all six nitrogens, while around Ru2 it is $2.133(22)$ Å for all five $Ru\text{--}NH_3$ distances. The bond involving the cyano nitrogen

(12) Matsubara, T.; Ford, P. C. *Inorg. Chem.* **1976**, *15*, 1107.

(13) Sheldrick, G. M. *SHELXS-97 and SHELXL-97: Programs for Structure Resolution and Refinement*; University of Göttingen: Göttingen, Germany, 1997.

(14) Sheldrick, G. M. *SHELXTL-PC*, version 5.0; Siemens Analytical X-ray Instruments, Inc.: Madison, WI, 1994.

(15) Allen, F. H.; Kennard, O. *Chem. Des. Autom. News* **1993**, *8*, 31.

(11) Juris, A.; Barigelletti, F.; Campagna, S.; Balzani, V.; Belser, P.; von Zelewski, A. *Coord. Chem. Rev.* **1988**, *84*, 85.

Table 3. Crystal and Structure Refinement Data for **2**

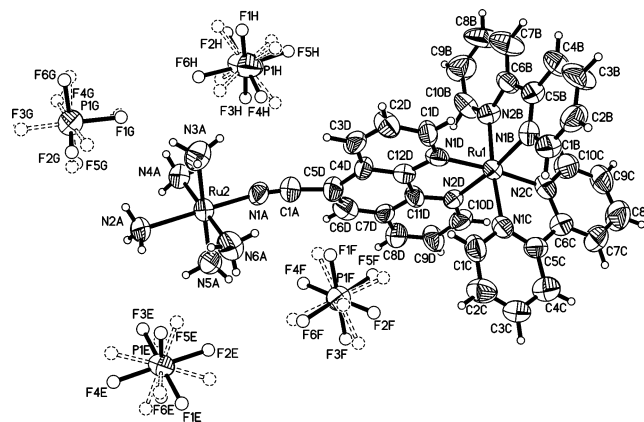
empirical formula	C ₃₃ H ₃₈ F ₂₄ N ₁₂ P ₄ Ru ₂
fw	1384.77
<i>T</i> (K)	293(2)
λ (Å)	0.710 73
cryst system	triclinic
space group	<i>P</i> 1
<i>a</i> (Å)	8.7270(15)
<i>b</i> (Å)	18.188(3)
<i>c</i> (Å)	18.924(3)
α (deg)	117.538(2)
β (deg)	97.221(3)
γ (deg)	92.838(3)
<i>V</i> (Å ³)	2622.5(8)
<i>Z</i>	2
<i>D</i> _{calc} (g cm ⁻³)	1.754
μ (mm ⁻¹)	0.823
<i>F</i> (000)	1368
cryst size (mm ³)	0.32 × 0.12 × 0.02
θ range (deg)	2.15–27.92
index ranges	–11 ≤ <i>h</i> ≤ 11, –23 ≤ <i>k</i> ≤ 20, 0 ≤ <i>l</i> ≤ 23
<i>N</i> _{tot} , <i>N</i> _{uniq} (<i>R</i> _{int}), <i>N</i> [<i>I</i> > 2 σ (<i>I</i>)]	21 438, 11 112 (0.085), 5390
params refined.	615
abs corr	semiempirical from equivalents
goodness-of-fit on <i>F</i> ²	0.825
final <i>R</i> indices [<i>I</i> > 2 σ (<i>I</i>)]	<i>R</i> 1 = 0.0725, <i>wR</i> 2 = 0.1983
<i>R</i> indices (all data) ^a	<i>R</i> 1 = 0.1689, <i>wR</i> 2 = 0.2535
$\rho_{\text{max}}/\rho_{\text{min}}$ in final ΔF (e Å ⁻³)	0.747 and –0.644

$$^a R1 = \sum ||F_o| - |F_c|| / \sum |F_o|; wR2 = [\sum [w(F_o^2 - F_c^2)^2] / \sum [w(F_o^2)^2]]^{1/2}.$$

Table 4. Selected Bond Lengths (Å) and Angles (deg) for **2**

Ru(1)–N(1D)	2.031(6)	Ru(2)–N(1A)	1.932(8)
Ru(1)–N(2B)	2.043(6)	Ru(2)–N(6A)	2.115(8)
Ru(1)–N(2C)	2.058(7)	Ru(2)–N(4A)	2.117(8)
Ru(1)–N(1B)	2.060(7)	Ru(2)–N(5A)	2.129(7)
Ru(1)–N(1C)	2.063(7)	Ru(2)–N(3A)	2.135(7)
Ru(1)–N(2D)	2.094(7)	Ru(2)–N(2A)	2.169(6)
N(1D)–Ru(1)–N(2B)	86.5(3)	N(1A)–Ru(2)–N(6A)	90.9(3)
N(1D)–Ru(1)–N(2C)	175.0(2)	N(1A)–Ru(2)–N(4A)	88.9(3)
N(2B)–Ru(1)–N(2C)	97.5(3)	N(6A)–Ru(2)–N(4A)	179.8(3)
N(1D)–Ru(1)–N(1B)	96.0(3)	N(1A)–Ru(2)–N(5A)	88.0(3)
N(2B)–Ru(1)–N(1B)	77.3(3)	N(6A)–Ru(2)–N(5A)	89.3(3)
N(2C)–Ru(1)–N(1B)	87.8(3)	N(4A)–Ru(2)–N(5A)	90.6(3)
N(1D)–Ru(1)–N(1C)	97.9(3)	N(1A)–Ru(2)–N(3A)	92.5(3)
N(2B)–Ru(1)–N(1C)	174.7(3)	N(6A)–Ru(2)–N(3A)	89.1(3)
N(2C)–Ru(1)–N(1C)	78.2(3)	N(4A)–Ru(2)–N(3A)	91.0(3)
N(1B)–Ru(1)–N(1C)	99.3(3)	N(5A)–Ru(2)–N(3A)	178.3(3)
N(1D)–Ru(1)–N(2D)	79.3(3)	N(1A)–Ru(2)–N(2A)	179.3(3)
N(2B)–Ru(1)–N(2D)	98.0(3)	N(6A)–Ru(2)–N(2A)	89.0(3)
N(2C)–Ru(1)–N(2D)	97.1(3)	N(4A)–Ru(2)–N(2A)	91.2(3)
N(1B)–Ru(1)–N(2D)	173.7(3)	N(5A)–Ru(2)–N(2A)	91.4(3)
N(1C)–Ru(1)–N(2D)	85.6(2)	N(3A)–Ru(2)–N(2A)	88.1(3)
C(1A)–N(1A)–Ru(2)	171.1(8)		

is distinctly shorter, 1.932(8) Å, due to the strong π -back-bonding from ammine ruthenium to the nitrile group. In effect, as reported by Creutz et al.,¹⁶ Ru–N(L) bond distances show large variations with L (from 2.06 Å for L = py to 1.95 Å for L = NCC₆H₅). Charge balance is achieved through a cloud of heavily disordered PF₆[–] anions which surround the dinuclear cations. They are preferentially located in the vicinity of Ru2 presenting seven units with their centers (the P atom) at distances lying between 5 and 5.40 Å from the metal, the next nearest P being at 9.4 Å. The bulky environment around Ru1 inhibits the anions to install too

**Figure 4.** Molecular diagram showing the numbering scheme used for complex **2**. In the disordered PF₆ units only the main moiety has been labeled.

near the cation, the nearest P being at 5.90 Å and the rest being well beyond 6.30 Å.

The closer approach between nonequivalent ruthenium atoms is found through the 5-CNphen bridge along the covalent link defining the molecule (Ru1...Ru2 = 9.503 Å). Equivalent rutheniums, however, lie closer (Ru1...Ru1[1 + *x*, *y*, *z*] = 8.727 Å; Ru2...Ru2[1 – *x*, –1 – *y*, 1 – *z*] = 8.394 Å).

The presence of a large number of eager H-bonding acceptors (24 independent fluorine atoms in the structure) causes a huge number of H...F short contacts to build up even in the absence of very acidic hydrogens. Table 5 (Supporting Information) presents the most important X–N...F interactions (X: N, C) subject to the (arbitrary) condition that the H...F distance be smaller than the sum of the corresponding van der Waals radii.

NMR Spectra. Figures 5–7 show the ¹H NMR spectrum of complex **1**, the H–H COSY spectrum of complex **1**, and the ¹H NMR spectrum of complex **2**, respectively, all in CD₃CN. Bidimensional techniques allowed the complete assignment of the signals, as shown in the Experimental Section.

In the mononuclear complex, ruthenium coordination put into evidence the magnetic inequivalence induced by the cyano group on the phenanthroline protons reported as multiplets in the free ligand 5-CNphen.^{5b} The most affected protons are H₄ and H₇, which are shifted to 8.80 and 8.70 ppm, respectively. Another consequence of ligand coordination to Ru(II) (which exerts a strong π -back-bonding effect) in complex **1** is the remarkable shielding of protons H₂ and H₉, which are displaced from 9.34 ppm to 8.25 and 8.23 ppm, respectively.

In the dinuclear complex **2**, the second metal coordination induces a shielding over all phenanthroline protons, with the exception of H₄ which is shifted to lower fields, indicating a barrier that avoids electronic circulation through it, an effect already observed in phenazine rings (such as dppz).

The protons of the 2,2'-bipyridine rings are slightly affected.

Photophysical Properties. All complexes prepared in this work emit at room temperature in acetonitrile at a wavelength

(16) Shin, Y. K.; Szalda, D. J.; Brunschwig, B. S.; Creutz, C.; Sutin, N. *Inorg. Chem.* **1997**, *36*, 3190.

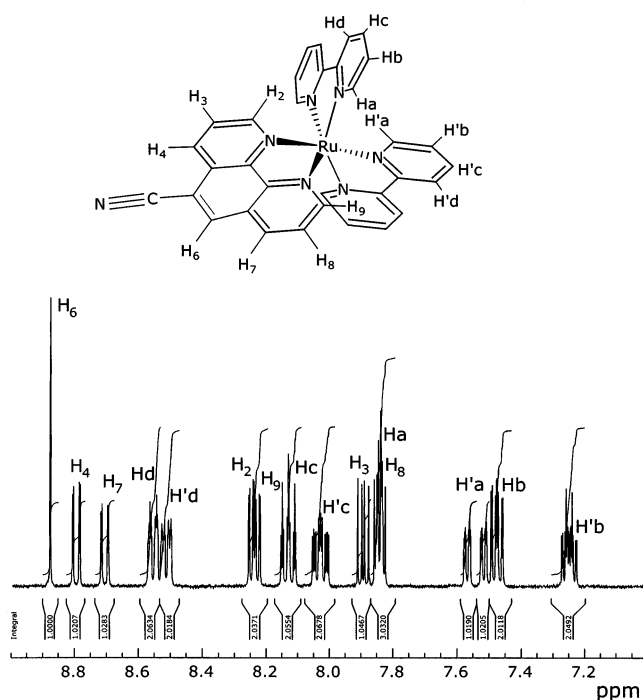


Figure 5. ^1H NMR spectrum of $[\text{Ru}(\text{bpy})_2(5\text{-CNphen})]^{2+}$, in CD_3CN .

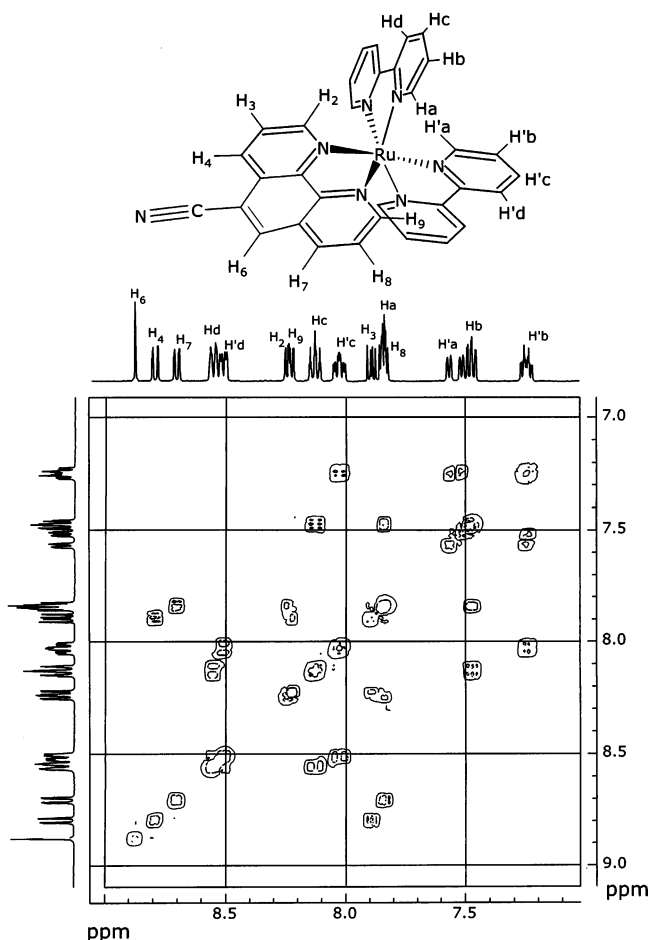


Figure 6. H-H COSY spectrum of $[\text{Ru}(\text{bpy})_2(5\text{-CNphen})]^{2+}$, in CD_3CN .

similar to other ruthenium polypyridine complexes¹¹ ($\lambda_{\text{em}} = 605 \text{ nm}$ at $\lambda_{\text{exc}} = 450 \text{ nm}$). However, the emission of the

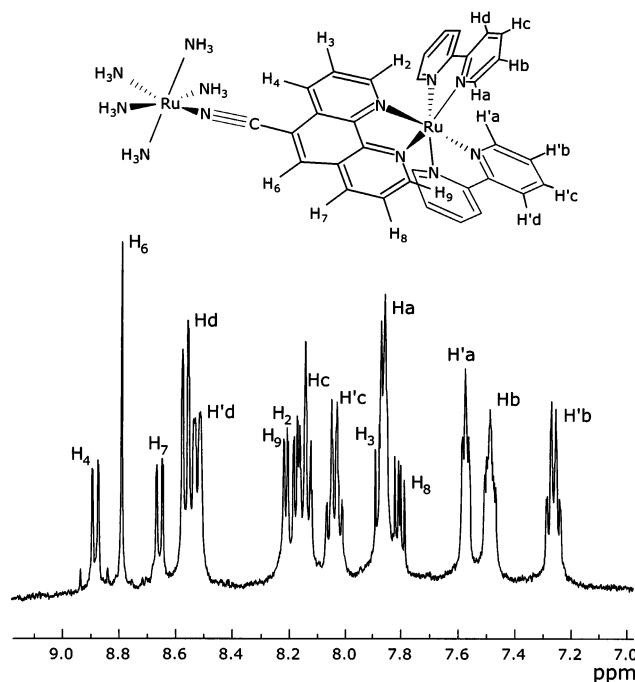


Figure 7. ^1H NMR spectrum of $[(\text{bpy})_2\text{Ru}^{\text{II}}(5\text{-CNphen})\text{Ru}^{\text{III}}(\text{NH}_3)_5]^{5+}$, in CD_3CN .

mononuclear parent complex **1** is quenched in both complexes **2** and **3**. Luminescence in the dinuclear species **2** is almost completely quenched, probably due to an autoabsorption effect (the ϵ values are much higher than the other two complexes at all visible wavelengths; see Table 1).

Figure 8 shows the luminescent spectra of complexes **1** and **3**. Quantum yields of 0.05 and 0.01 for complexes **1** and **3**, respectively, were determined^{17a} by

$$\phi_2 = \phi_1(I_2/I_1)(n_2/n_1)^2(A_1/A_2) \quad (1)$$

where ϕ is the emission quantum yield of either known (1) or unknown (2) ($\phi_1 = 0.062$ was taken for $[\text{Ru}(\text{bpy})_3]^{2+}$ in acetonitrile),^{17b} I is the integrated sum of the emission intensity (area under the emission maximum), A is the absorbance at λ_{exc} in a 1-cm cell, and n is the refractive index of the solvent (assumed as approximately equal to that of the solution).

The emission of **3** cannot be attributed to impurity traces, since the same results were obtained when dissolving the pure solid sample or when oxidizing complex **2** "in situ". While complex **1** behaves as a photosensitizer as good as $[\text{Ru}(\text{bpy})_3]^{2+}$, there is a significant quenching in the luminescence (by a factor of 5) in the mixed-valent species **3**, indicating possible intramolecular electron-transfer processes taking place after light excitation of the mixed-valent Ru(II)–Ru(III) dimer, as shown in Scheme 1. In this scheme, $h\nu$ is the excitation photon, $h\nu'$ is the emission photon, k_q is the rate constant for the quenching process (assumed as a very rapid step), k_b is the rate constant for the charge recombination step, and MMCT is the absorption process

(17) (a) Jones, W. E., Jr.; Bignozzi, C. A.; Chen, P.; Meyer, T. J. *Inorg. Chem.* **1993**, *32*, 1167. (b) Caspar, J. V.; Meyer, T. J. *J. Am. Chem. Soc.* **1983**, *105*, 5583.

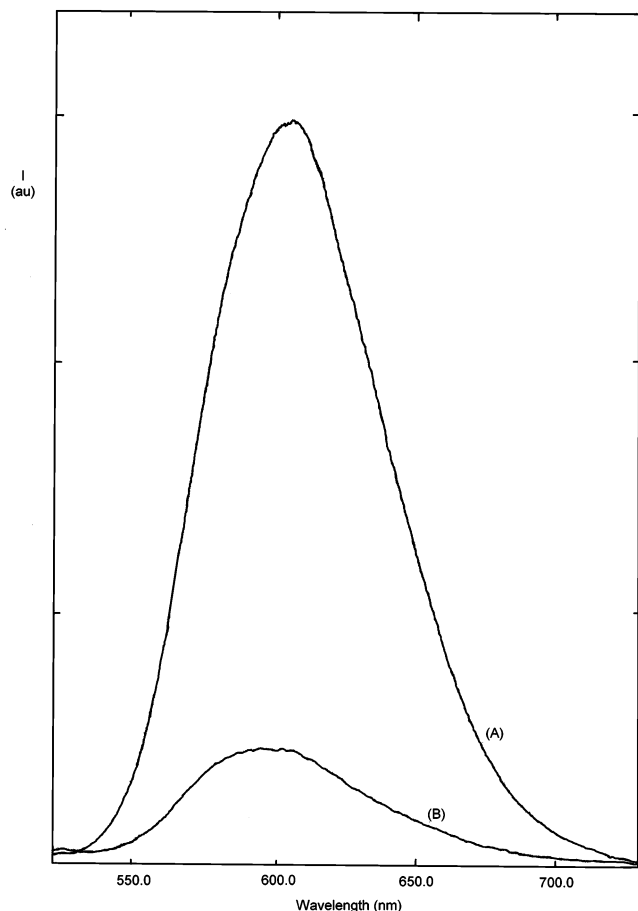
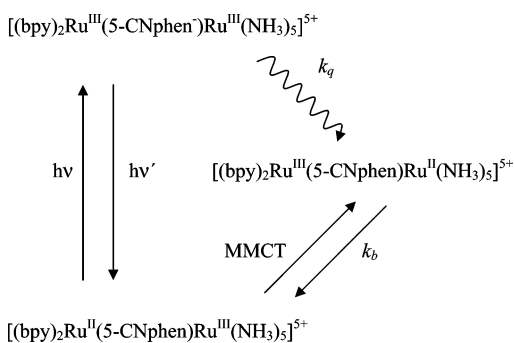


Figure 8. (A) Emission spectrum of complex $[\text{Ru}(\text{bpy})_2(5\text{-CNphen})]^{2+}$. (B) Emission spectrum of $[(\text{bpy})_2\text{Ru}^{\text{II}}(5\text{-CNphen})\text{Ru}^{\text{III}}(\text{NH}_3)_5]^{5+}$. Both solutions have equal absorbances in CH_3CN , at $\lambda_{\text{exc}} = 450$ nm, and $T = 22$ °C.

Scheme 1



described before. This complex is thus a good model for testing current electron transfer theories, if the rate constant k_b could be measured by accessible laser techniques. From the spectral data for the MMCT band, we could predict this value by resorting to the Marcus–Hush formalism, as discussed below.

Intramolecular Electron Transfer. The properties of the mixed-valent ($\text{Ru}_b^{\text{II}}\text{—Ru}_a^{\text{III}}$) complex were analyzed within the context of the Marcus–Hush model. The experimental values of $\Delta\tilde{\nu}_{1/2}$, ϵ_{max} , and E_{op} , obtained by deconvolution of the broad-Gaussian-shaped MMCT band shown in Figure 3, were applied in the estimation of H_{AB} , α^2 , and λ (the electronic coupling, the electron delocalization parameter,

and the reorganization energy for the intramolecular electron transfer, respectively) through eqs 2–4:¹⁸

$$H_{\text{AB}} \text{ (in cm}^{-1}\text{)} = 2.06 \times 10^{-2} [(\epsilon_{\text{max}})(\tilde{\nu}_{\text{max}})(\Delta\tilde{\nu}_{1/2})]^{1/2} (1/r) \quad (2)$$

$$\alpha^2 = (H_{\text{AB}}/\tilde{\nu}_{\text{max}})^2 \quad (3)$$

$$\lambda = E_{\text{op}} - \Delta G^\circ - \Delta E_{\text{exc}} \quad (4)$$

Here r is the distance between both metal centers (in Å), ϵ_{max} is the molar absorptivity (in $\text{M}^{-1} \text{cm}^{-1}$), $\Delta\tilde{\nu}_{1/2}$ is the bandwidth at half-height (in cm^{-1}), $\tilde{\nu}_{\text{max}}$ is the maximum absorption frequency of the MMCT band (in cm^{-1}), E_{op} is the energy of the intervalence absorption maximum (in eV), ΔG° is the free energy between both redox centers, assumed as approximately $\Delta E_{1/2}$ (see section of Electrochemical Measurements), and ΔE_{exc} is the energy difference between the excited and ground states, estimated as 0.25 (eV) for several ruthenium complexes in the event that MMCT results in the population of an excited state.¹⁹ The value of the metal-to-metal distance r ($=9.5$ Å) was determined by X-ray diffraction (see X-ray section) and is consistent with crystallographic data of model compounds.^{16,20}

Equation 4 gives a calculated value of $\lambda = 0.93$ eV, which is greater than $-\Delta G^\circ$ ($=0.70$ V) for the charge recombination process $\text{Ru}_a^{\text{II}} \rightarrow \text{Ru}_b^{\text{III}}$; therefore, according to Marcus theory,²¹ the rate constant k_b for this step (shown in Scheme 1) should fall in the normal region but close to the barrierless region and so predicted to be rapid. Efforts to measure k_b experimentally will be done soon. The magnitudes of H_{AB} and α^2 were determined by eqs 2 and 3 to be 190 cm^{-1} and 1.6×10^{-4} , respectively, suggesting that although there is a detectable electron coupling between both metallic centers through the bridging N-heterocyclic ligand, the extension of this interaction is relatively weak, as expected by the considerable distance between donor and acceptor. Consequently, this system can be best described as belonging to class II (moderate coupling), of Robin and Day's categorization.¹⁸

Conclusions. The new mononuclear complex described here is a good photosensitizer that can be used as a precursor for polynuclear molecular entities that may engage in light-induced electron-transfer processes. We demonstrate here in particular that 5-cyano-1,10-phenanthroline can bridge two ruthenium atoms with a slight electronic coupling at a considerable distance. The redox asymmetry and the moderate reorganization energy results in a charge recombination process close to the barrierless region. The mixed-valent system described in this work is thus a good model for testing current electron-transfer theories.

Acknowledgment. Support from a SETCIP (Argentina)–CONYCIT (Chile) agreement is gratefully acknowledged. M.G.M. thanks CONICET (Argentina) for a graduate fellowship. F.F. and N.E.K. are Members of the Research

(18) Creutz, C. *Prog. Inorg. Chem.* **1983**, 30, 1.

(19) Katz, N. E.; Creutz, C.; Sutin, N. *Inorg. Chem.* **1988**, 27, 1687.

(20) Goldstein, B. M.; Barton, J. K.; Berman, H. M. *Inorg. Chem.* **1986**, 25, 842.

(21) Marcus, R. A.; Sutin, N. *Biochim. Biophys. Acta* **1985**, 811, 265.

Career (CONICET) and thank CIUNT and CONICET for financial support. M.T.G. and R.B. are grateful for funding by CONICYT-FONDAP (Grant No. 11980002). Support from CONICYT (Doctoral Thesis support to A.D.) and FONDECYT (Líneas Complementarias 8980007 and Project 1020517) is also acknowledged.

Supporting Information Available: Crystallographic data in CIF format and Table 5 (H-bonding interactions of complex **2**).

This material is available free of charge via the Internet at <http://pubs.acs.org>. Crystallographic data (excluding structure factors) have been deposited with the Cambridge Crystallographic Data Centre as supplementary publication No. CCDC 219918. Copies of the data can be obtained free of charge on application to the CCDC, 12 Union Road, Cambridge CB2 1EZ, U.K. (fax (44) 1223 336–033; E-mail deposit@ccdc.cam.ac.uk).

IC035198D